

EXPERIMENTAL AND NUMERICAL ANALYSIS OF AIRFLOW IN A SURGICAL ROOM

Danilo de Moura, danilo.moura2@poli.usp.br

Victor Barbosa Felix, victor.felix@poli.usp.br

Escola Politécnica da Universidade de São Paulo - Programa de Pós Graduação em Engenharia Mecânica-Av. Prof. Mello Moraes, 2231, 05508-900 - São Paulo - SP

Marcelo Luiz Pereira, marcelo@sj.cefetsc.edu.br

CEFETSC/SJ - Centro Federal de Educação Tecnológica de Santa Catarina, Rua José Lino Kretzer, 608 - Praia Comprida- 88103-902 - São José - SC - Brasil

Escola Politécnica da Universidade de São Paulo - Programa de Pós Graduação em Engenharia Mecânica-Av. Prof. Mello Moraes, 2231, 05508-900 - São Paulo - SP

Arlindo Tribess, atribess@usp.br

Escola Politécnica da Universidade de São Paulo, Departamento de Engenharia Mecânica - Av. Prof. Mello Moraes, 2231, 05508-900- São Paulo - SP

Abstract. *Owing the great importance in the health, well to be and effectiveness of the work of the surgical team, every day the concern with air quality and thermal comfort conditions in surgical rooms is increasing. The airflow velocities and temperatures are the main parameters that describe the air movement inside the environment and influence directly in the quality of the air and in the conditions of thermal comfort in surgical rooms. The temperature and velocity fields permit us to verify if the air distribution is homogeneous or if occur stagnation and turbulence areas or thermal gradients; which helps the formation of drafts along the room that influence in the movement of the particles and, consequently, in the control of infections during the surgery. The work was developed at a surgical room where parameters that characterize the environment were measured and simulated for the numerical analysis. For the numerical simulation the commercial softwares Icem and Fluent were used for the generation of the mesh and to simulate the airflow inside the surgical room, respectively. For the experimental study anemometers and thermometers were distributed along the room. Results of numerical simulation were compared with experimental data. Good agreement was verified in the results of the air behaviour in the simulation and in the experimental work. The temperatures remain practically uniform and stagnation zones were observed.*

Keywords: *Indoor air quality, airflow, computational fluid dynamic, surgical rooms.*

1. INTRODUCTION

Surgical rooms constitute complex environments that request appropriate ventilation to reduce the risks of the patient's infection and of the professionals' health by airborne particles. No less important, the conditions of the surgeon's thermal comfort and of the medical team need to be the best as possible so that they work in favorable conditions for the success of the surgical procedure.

The airflow velocities and temperatures influence directly the air quality and the environmental conditions for thermal comfort achievement. The modeling techniques for numerical simulation of the airflow behavior in surgical rooms have been object of a great number of investigations, although the variety of possible cases turns it an area with need of endless studies for the evaluation of ventilation and air quality conditions. Chow and Yang (2003) present a revision on the state-of-art of ventilation studies in surgical rooms, showing that applied numerical methods began to appear in 1990 with the growth of mathematical and computational modeling.

Since then, the use of computational fluid dynamics (CFD) technique is becoming a very powerful and efficient tool in studies of the behavior of drafts and dispersion of pollutants in ventilated environments (Chen et al, 1992; Hartung and Kluger, 1998; Memarzadeh and Jiang, 2001; Memarzadeh and Manning, 2002; Chow and Yang, 2003; Kameel and Khalil, 2003; Liu and Moser, 2002; Wloszyn et al., 2003; Memarzadeh and Jiang, 2004; Tung and Hu, 2004; Kao and Yang, 2005). Besides, processes of numerical simulation using CFD are a form to evaluate the performance of ventilation systems in the control of particles (Memarzadeh and Jiang, 2002; Chow and Yang, 2003; Liu et al., 2003; Wloszyn et al., 2003; Memarzadeh and Jiang, 2004; Tung and Hu, 2004; Kao and Yang, 2005).

With the use of CFD the following questions can be answered: in which place of the room the surgical table should be installed, which are the appropriate changes of air, which air supply and return system should be chosen and if the level of cleaning of the room was obtained.

Chen et al (1992) were of the first ones to accomplish, with success, the numerical simulation of the airflow and of the concentration of particles in a surgical room. According to the authors, the sources of heat possess little effect in the distribution of particles and in the thermal comfort in a surgical room. As some authors, the airflow in the sterilized area is basically unidirectional, but in areas out of the surgical field it is basically turbulent (Chen et al, 1992; Hartung and Kluger, 1998; Memarzadeh and Jiang, 2001).

The use of CFD technique to evaluate the influence of the architecture and position of equipments in surgical rooms is being used and it is demonstrating to be an excellent tool for this kind of evaluation. Chow and Yang (2003) applied CFD to evaluate a surgical room with the objective of verifying the influence of the surgical focus and of auxiliary lamps in the distribution of pollutants. Memarzadeh and Jiang, (2004) used CFD to analyze the performance of the ventilation system in a surgical room with different architectures and results were compared with experimental data showing satisfactory agreement.

Liu et al (2002) affirm that although experimental approaches are relatively cheap, it is not possible to capture some details of the airflow with instruments. These authors evaluated a surgical room in a hospital with the objective of verifying the best architecture and layout of some components in the room using CFD technique. The influence in particle distribution was analyzed.

The air supply is a fundamental parameter for temperature control and distribution of pollutants in the environment. Wloszyn et al. (2003) studied the airflow and distribution of particles using experimental and numerical methods in isothermal conditions. According experimentation and simulation results, these authors concluded that the risk of contamination is directly influenced by the air inlet and outlet positions, room geometric parameters and the source of pollutants emission. Kao and Yang (2005) also analyzed different air supply and air return systems to verify the efficiency of removal of pollutants in the surgical field. As other mentioned authors, they also observed that the disposition of diffusers and of return grilles have a great influence in the airborne movement inside the room.

This paper presents the results of experimental and numerical simulation results of airflow and temperature conditions in a surgical room with turbulent ventilation system. The objective was to evaluate the influence of the architecture, layout of equipments and ventilation system on the room airflow conditions.

2. ROOM ARCHITECTURE AND AIR DISTRIBUTION CONFIGURATION

In the present study the room has rectangular form with 6.20 x 5.80 x 3.15m and contains a surgical table, four auxiliary tables for utensils, a surgical focus and anesthesia equipment. The ventilation system consists on a single inlet diffuser located at the superior side of the wall with an outlet grille in the opposite inferior side of the same wall. The diffuser supplies an unidirectional jet of air in the environment. The room architecture, the layout of equipment and details of the air supply system are shown in Fig. 1.

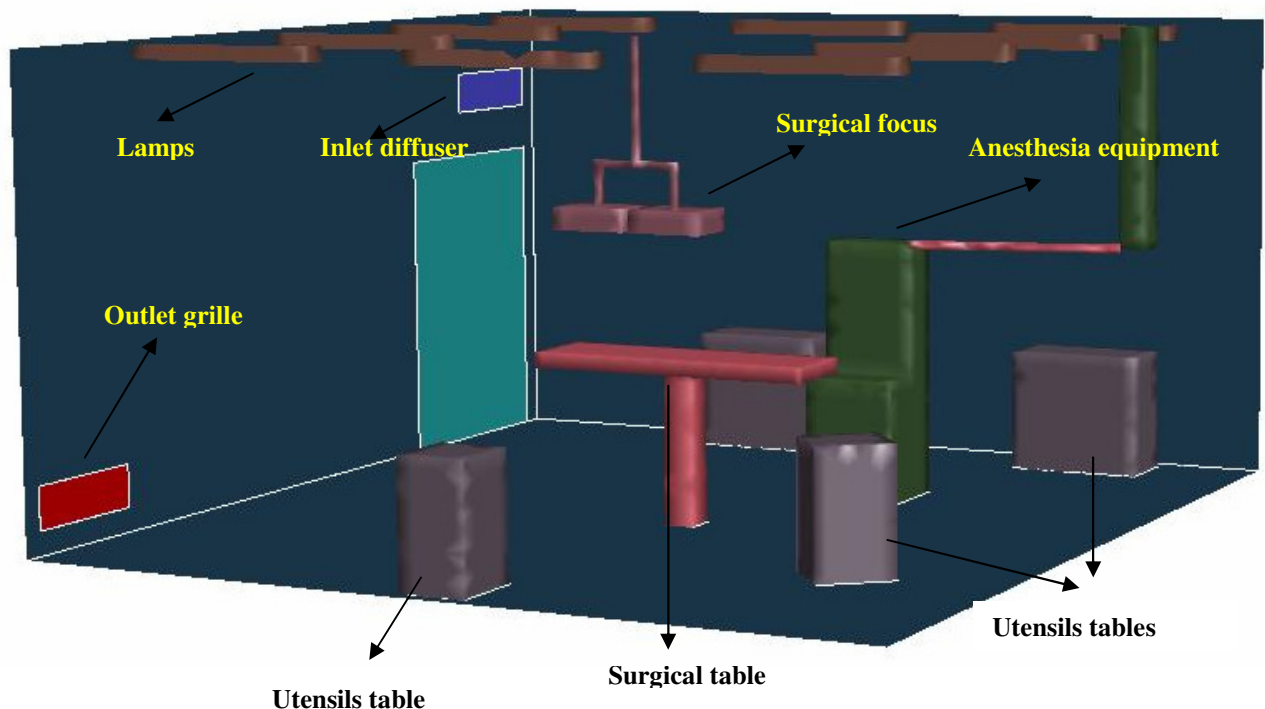


Figure 1. Surgical room architecture, layout of equipment and air supply system.

3. EXPERIMENTAL PROCEDURE

The experimental procedure was accomplished with the surgical room in acclimatized steady state environment conditions without people. Environment conditions were evaluated using four pedestals, with air temperature and velocity sensors, positioned at the surgical room as shown in Fig. 2. Each one of the pedestals contains four sensors of air temperature and four omni directional anemometers located at the heights of: 0.60; 1.21; 1.80 and 2.40m from the floor. A pedestal with only one sensor of temperature and of velocity was positioned at the top of the surgical table, 1.5m from the floor.

For the simulation process needs, measurements of inlet airflow conditions and of superficial temperatures of lamps and of the surgical focus were also carried out. For that a bolometer, a thermometer and a laser temperature meter were used. Characteristics of the measuring instruments are shown in Tab. 1.

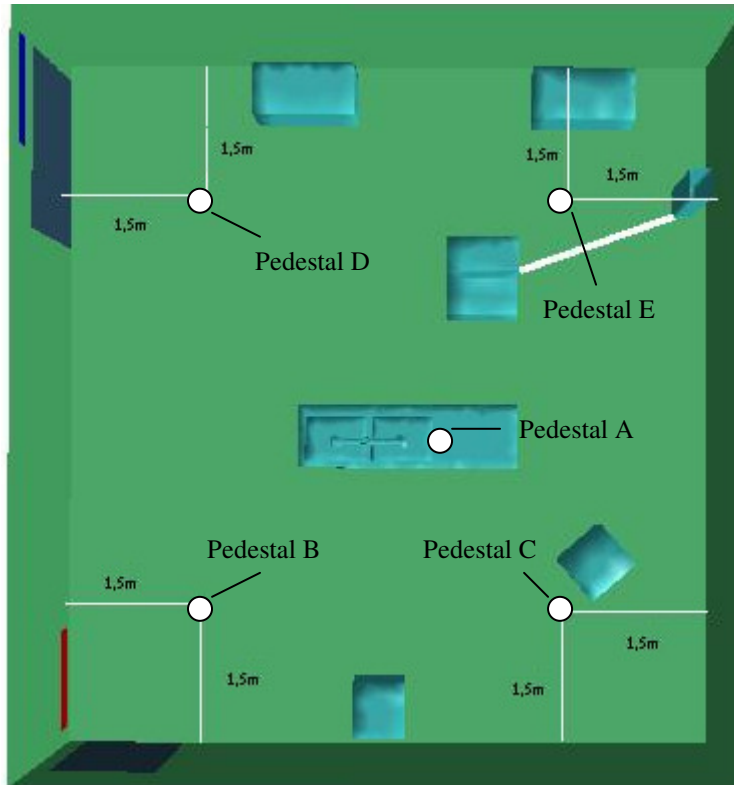


Figure 2. Points of measuring air temperatures and velocities

Table 1. Characteristics of the measuring instruments

| Quantity | Measuring range | Accuracy |
|---|-----------------|------------------|
| Air temperature, °C | 10 a 40 | ± 0.2 °C |
| Superficial temperature, °C | 10 a 200 | ± 0.1 °C |
| Air velocity (for environment measurements), m/s | 0 a 1 | ± (0.04 + 3% Va) |
| Air flow (for diffuser measurements), m ³ /h | 85 a 4078 | ± (3% Qa) |

3. MATHEMATICAL EQUATIONS

The following equations (Eq. (1) to Eq.(4)) were used to solve the airflow in ventilated environments. Equation (1) is the continuity equation.

$$\frac{\partial \rho}{\partial t} + \text{div}(\rho \vec{u}) = 0$$

where ρ is the specific mass and \vec{u} is the velocity vector.

Equation (2) is the momentum equation in cartesian coordinates.

$$\frac{\partial}{\partial t}(\rho u) + \text{div}(\rho \bar{u}\bar{u}) = -\text{grad } p + \text{div}(\tau_{\text{eff}}) + \rho \bar{g} + \bar{F}$$

where g is the gravity, p is the pressure and F are forces. (2)

Equation (3) represents the effective tensor stress.

$$\tau_{\text{eff}} = (\mu + \mu_t) \left(\frac{\partial u_i}{\partial x_j} + \frac{\partial u_j}{\partial x_i} \right) - \frac{2}{3} \rho k \delta_{ij}$$

where μ is the molecular viscosity, μ_t is the turbulent viscosity, k is the turbulent kinetic energy and δ_{ij} is the Kronecker delta.

Equation (4) represents the energy equation, where k_{eff} is the effective conductivity, Φ is the viscous work, T is the temperature and S_e is a source term.

$$\frac{\partial \rho e}{\partial t} + \text{div}(\rho e \bar{u}) = -p \text{div}(\bar{u}) + \text{div}(k_{\text{eff}} \text{grad } T) + \Phi + S_e$$

To solve the turbulence in the flow the k-ε standard model was used and equations can be found in Fluent (2003).

4. SIMULATION PROCEDURE

Initially three meshes were generated for the comparison of numerical and experimental results. These meshes differ only by the refinement degree (Tab. 2) and were obtained using commercial program ICEM.

Table 2. Number of elements of the tetrahedral meshes.

| Mesh | Number of elements (million) |
|------|------------------------------|
| 1 | 303 |
| 2 | 612 |
| 3 | 1015 |

4.1. Simulation boundary conditions

Turbulent airflow in steady state conditions was considered. The gravity was taken into account with value of 9.8 m/s². To simulate natural convection was used the Boussinesq ideal gas model and coefficient of thermal expansion equal to 10⁻⁵ K⁻¹. The other values and boundary conditions were presented in Tab. 3:

Table 3. Boundary conditions.

| | Boundary condition |
|----------------------------------|---|
| Diffuser | Air mass flow of 0.787 kg/s and air temperature of 17.6°C |
| Outlet grille | Gauge pressure of 0 Pa |
| Lamps | Superficial temperature of 30.0 °C |
| Surgical focus | Superficial temperature of 45.0 °C |
| Walls, roof, floor and furniture | Adiabatic condition |

4.2. Convergence criterion.

As convergence criterion were considered residues in the order of 10^{-6} , with a maximum of 2.000 iterations, for the equations of continuity, velocity, energy and k-ε. Initial conditions of null velocities in the coordinates (x, y, z) and temperature of 300 K were imposed. The numerical schemes used to solve the conservation equations and other auxiliary equations were of second order.

4.3. Comparison between numerical and experimental results.

For the analysis of the most adequate mesh, values of temperature and velocities were used to compare simulation and experimental results. For that, experimental values of temperatures and velocities measured using the pedestals B, C, D and E (Fig. 2) were considered. The comparison results are presented in Figs. 3 and 4 and in Tabs 4 and 5, for temperatures, and in Figs. 5 and 6 and in Tabs. 6 and 7, for velocities.

Analyzing the results presented in Figs. 3, 4, 5 and 6 and in Tabs. 4, 5, 6 and 7, it can be observed that:

- The simulation results of temperature and velocities do not present significant variations between meshes.
- The simulation results present good agreement with the experimental data and that the temperature values present better results than the velocity ones. It can be verified that the experimental values of velocities in the pedestal D, in the heights of 1.80m and 2.40m, present much larger results than that of simulation, and in the pedestal E these results are smaller than that obtained by simulation. This should be due to an inclination (down direction) in the air supply diffuser, no appropriately considered in the simulation process.
- The mesh 1 presents good results with smaller computational time: about 35% in relation to mesh 2 and 60% in relation to mesh 3. So, this mesh was considered the best mesh.

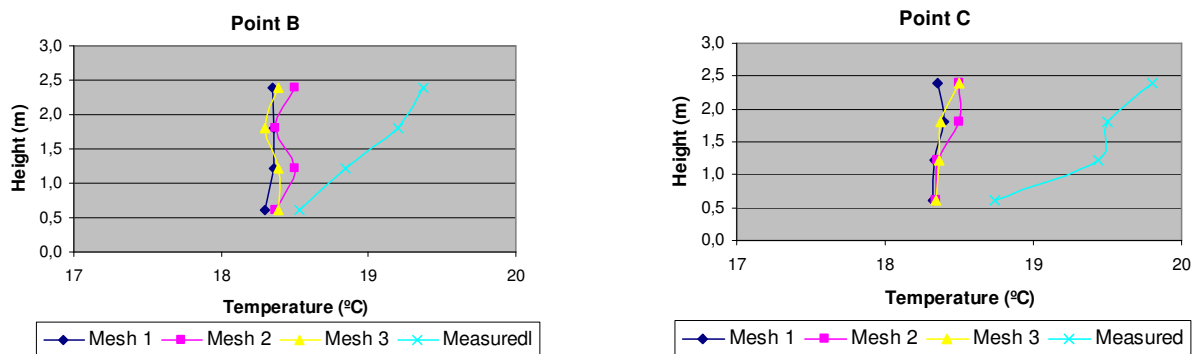


Figure 3. Comparison between numerical and experimental air temperature results (pedestals B and C).

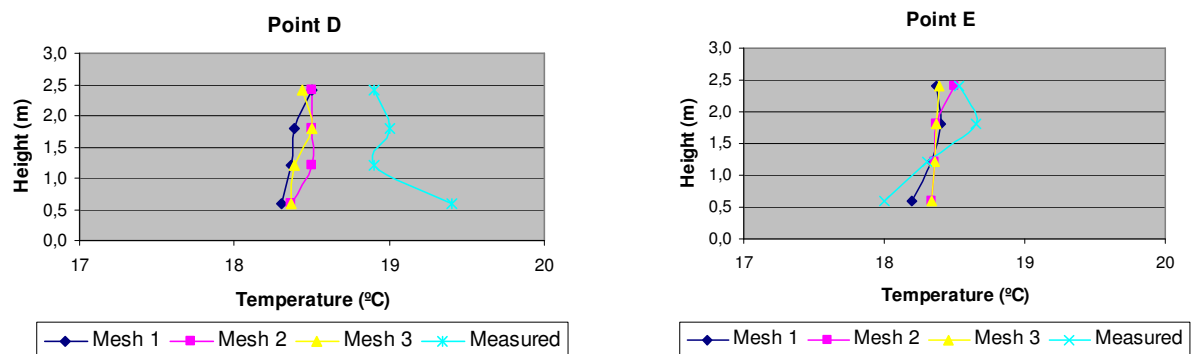


Figure 4. Comparison between numerical and experimental air temperature results (pedestals D and E).

Table 4. Numerical and experimental air temperature results (pedestals B and C).

| TEMPERATURE POINT B (°C) | | | | | TEMPERATURE POINT C (°C) | | | |
|--------------------------|------|------|------|---------------|--------------------------|------|------|------|
| 0.60 | 1.21 | 1.80 | 2.40 | Height (m) | 0.60 | 1.21 | 1.80 | 2.40 |
| 18.3 | 18.4 | 18.4 | 18.3 | Mesh 1 (°C) | 18.3 | 18.3 | 18.4 | 18.4 |
| 18.4 | 18.5 | 18.4 | 18.5 | Mesh 2 (°C) | 18.3 | 18.4 | 18.5 | 18.5 |
| 18.4 | 18.4 | 18.3 | 18.4 | Mesh 3 (°C) | 18.3 | 18.4 | 18.4 | 18.5 |
| 18.5 | 18.8 | 19.2 | 19.4 | Measured (°C) | 18.7 | 19.4 | 19.5 | 19.8 |

Table 5. Numerical and experimental air temperature results (pedestals D and E).

| TEMPERATURE POINT D (°C) | | | | | TEMPERATURE POINT E (°C) | | | |
|--------------------------|------|------|------|------------|--------------------------|------|------|------|
| 0.60 | 1.21 | 1.80 | 2.40 | Height (m) | 0.60 | 1.21 | 1.80 | 2.40 |
| 18.3 | 18.4 | 18.4 | 18.5 | Mesh 1 | 18.2 | 18.3 | 18.4 | 18.4 |
| 18.4 | 18.5 | 18.5 | 18.5 | Mesh 2 | 18.3 | 18.4 | 18.4 | 18.5 |
| 18.4 | 18.4 | 18.5 | 18.4 | Mesh 3 | 18.3 | 18.4 | 18.4 | 18.4 |
| 19.4 | 18.9 | 19.0 | 18.9 | Measured | 18.0 | 18.3 | 18.7 | 18.5 |

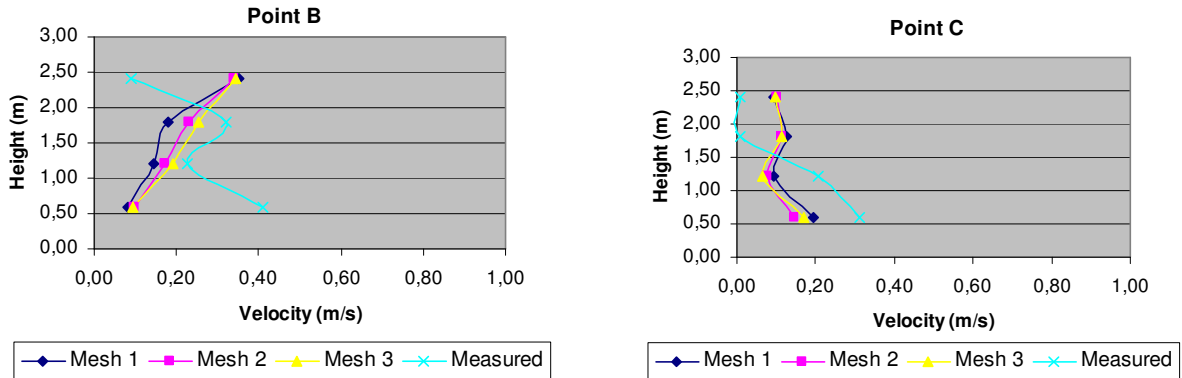


Figure 5. Comparison between numerical and experimental air velocity results (pedestals B and C).

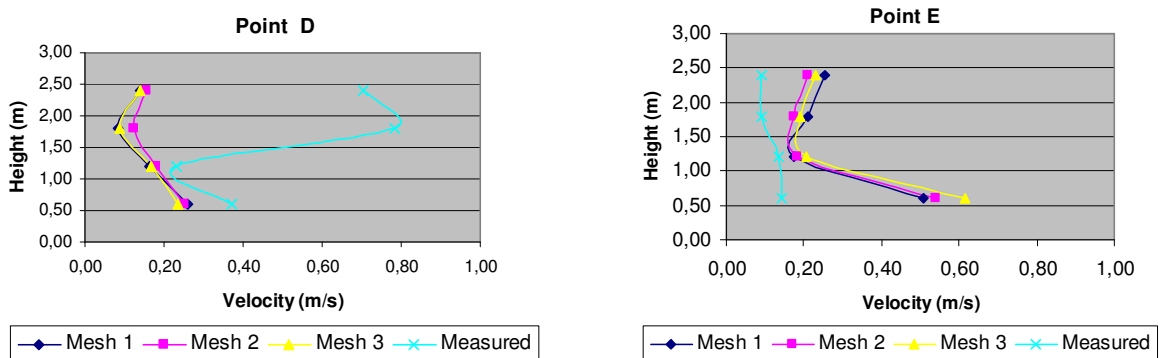


Figure 6. Comparison between numerical and experimental air velocity results (pedestals D and E).

Table 6. Numerical and experimental air velocity results (pedestals B and C).

| VELOCITY POINT B (m/s) | | | | | VELOCITY POINT C (m/s) | | | |
|------------------------|------|------|------|------------|------------------------|------|------|------|
| 0.60 | 1.21 | 1.80 | 2.40 | Height (m) | 0.60 | 1.21 | 1.80 | 2.40 |
| 0.08 | 0.15 | 0.18 | 0.35 | Mesh 1 | 0.19 | 0.09 | 0.13 | 0.09 |
| 0.10 | 0.17 | 0.23 | 0.34 | Mesh 2 | 0.15 | 0.08 | 0.11 | 0.10 |
| 0.09 | 0.19 | 0.26 | 0.34 | Mesh 3 | 0.17 | 0.06 | 0.11 | 0.10 |
| 0.41 | 0.23 | 0.32 | 0.09 | Measured | 0.31 | 0.21 | 0.01 | 0.01 |

Table 7. Numerical and experimental air velocity results (pedestals D and E).

| VELOCITY POINT D (m/s) | | | | | VELOCITY POINT E (m/s) | | | |
|------------------------|------|------|------|--------------|------------------------|------|------|------|
| 0.60 | 1.21 | 1.80 | 2.40 | Height (m) | 0.60 | 1.21 | 1.80 | 2.40 |
| 0.26 | 0.16 | 0.09 | 0.14 | Mesh 1 | 0.51 | 0.18 | 0.21 | 0.25 |
| 0.25 | 0.18 | 0.13 | 0.16 | Mesh 2 | 0.54 | 0.18 | 0.18 | 0.21 |
| 0.24 | 0.17 | 0.09 | 0.14 | Mesh 3 | 0.62 | 0.21 | 0.19 | 0.23 |
| 0.37 | 0.23 | 0.78 | 0.71 | Measured | 0.14 | 0.14 | 0.09 | 0.09 |

5. SIMULATION RESULTS

For the presentation of simulation results the mesh 1 (Fig. 7) was chosen due to its best performance in comparison with experimental data, presented in the item 4.3.

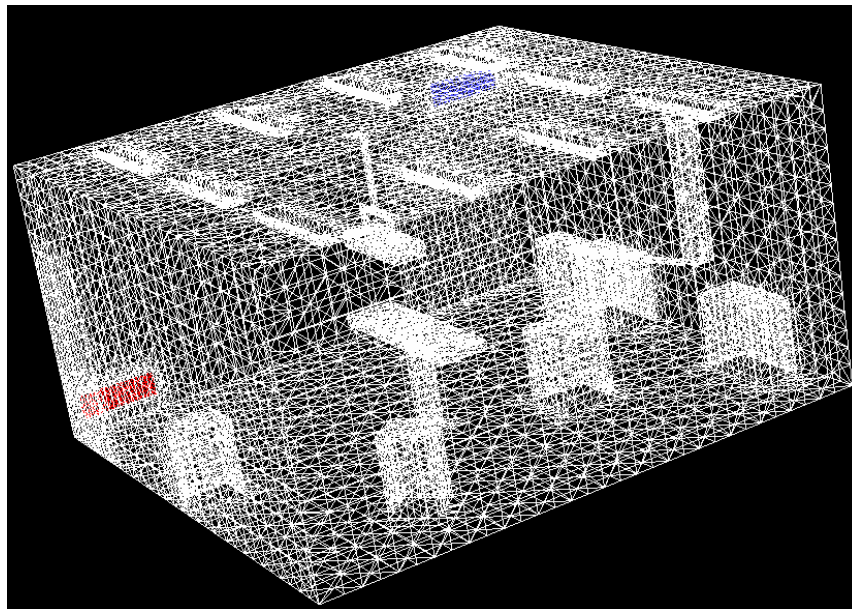


Figure 7. Tetrahedral mesh with 303 million elements.

The surgical field is the area of greater interest in a surgical room. Like this, for the presentation of numerical results the room was divided in 2 plans that cross the area of the surgical field: plan X = 3.2m and plan Z = -3.0m. So, with the presentation of results in these plans the behavior of the airflow and temperature distribution in this area can be verified.

5.1. Air temperatures

The numerical results of air temperatures at the planes crossing the surgical field are presented in Fig. 8. One can observe that results presented in Fig. 8 show correctly higher temperatures near the surgical field caused by the heat dissipated by the surgical focus. A higher temperature was also verified in the experimental evaluation in the center of the surgical field, 0.5m above the surgical table, with a temperature of 20.2 °C. The other areas present a practically uniform temperature; which was also observed in the temperature measuring results presented in the item 4.3.

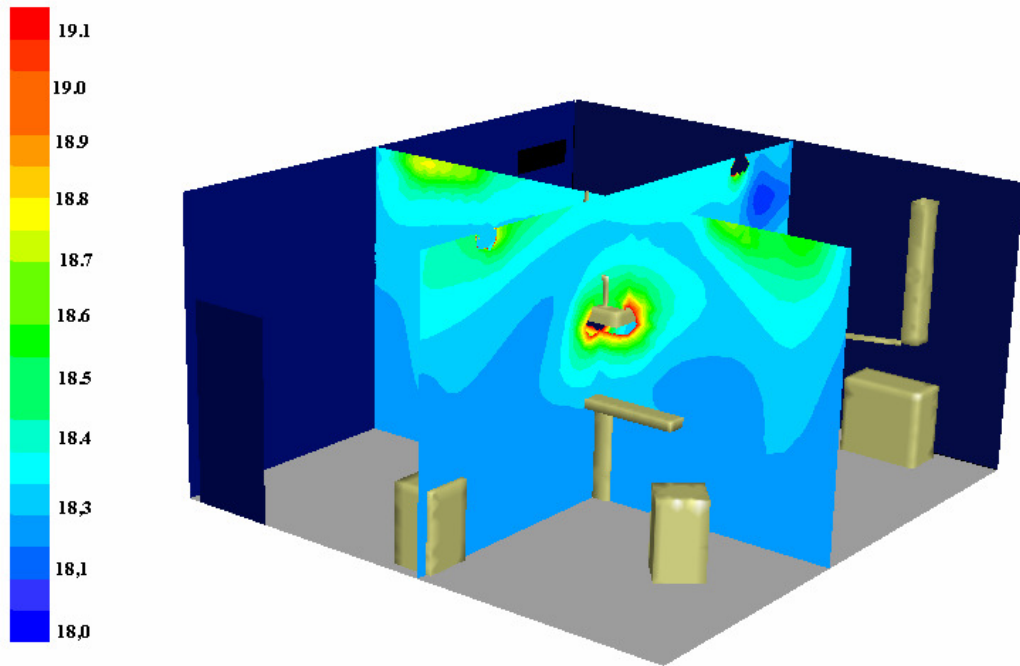


Figure 8. Air temperatures at the planes crossing the surgical field.

5.2. Air velocities.

Numerical results of air velocities and velocity vectors at the planes crossing the surgical field are presented, respectively, in Figs. 9 and 10.

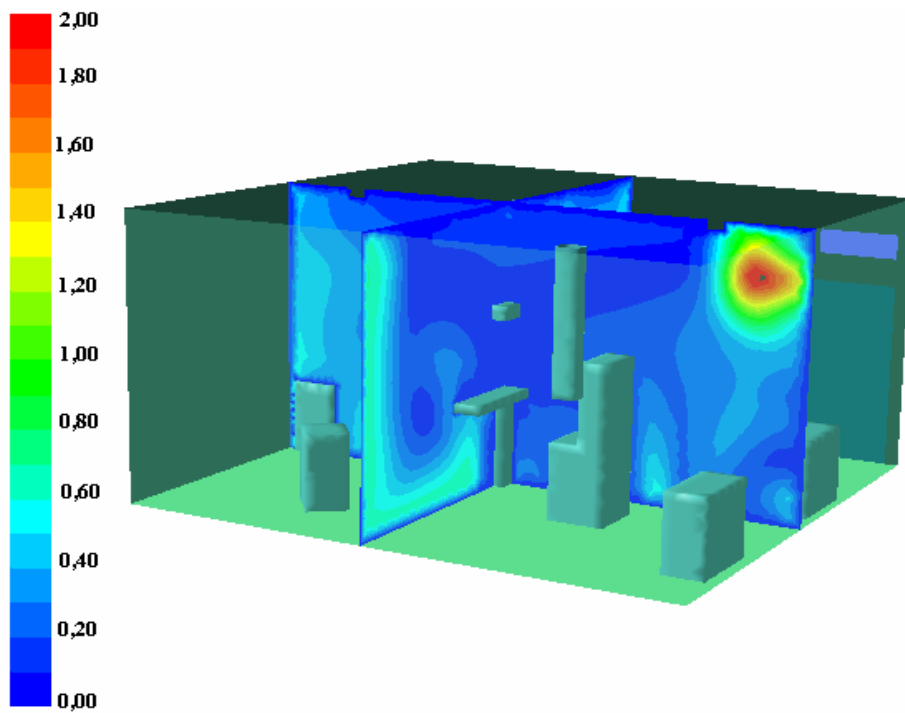


Figure 9. Air velocities at the planes crossing the surgical field.

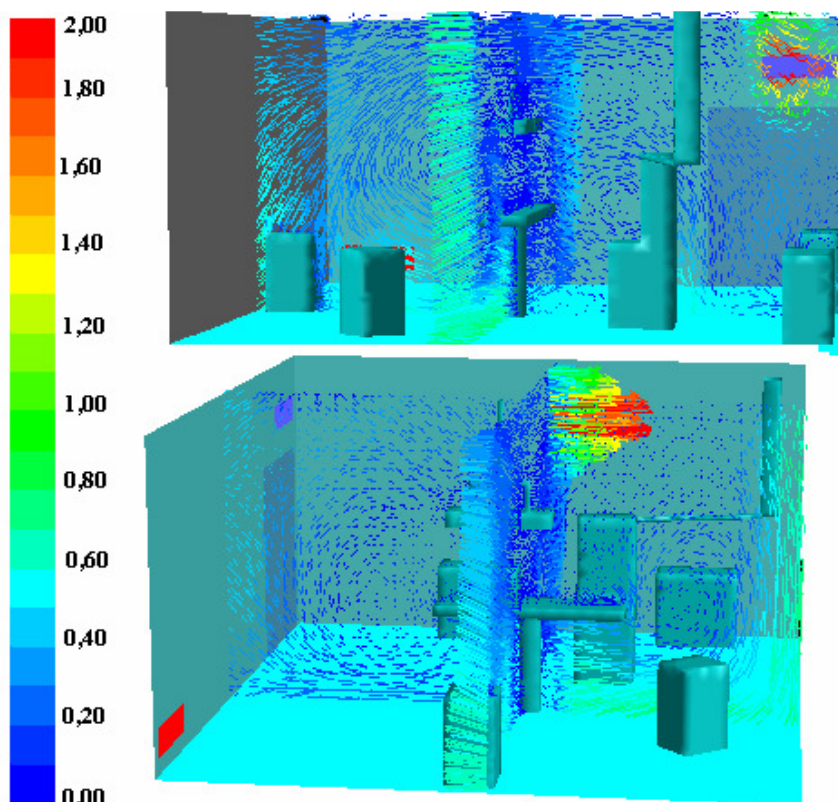


Figure 10. Velocity vectors at the planes crossing the surgical field.

In Figure 9 it can be observed very low velocities and stagnation in the surgical field area. Air velocity measured in the surgical field (pedestal A) of the order of 0.01 m/s corroborated the numerical results.

Finally, Figure 10 shows recirculation areas near the surgical field, which can aid in the resuspension of airborne particles and contaminate the surgical wound.

6. CONCLUSION

Experimental and numerical simulation studies were accomplished at a surgical room. The numerical results presented good agreement with the experimental ones and showed that the surgical room presents a practically homogeneous temperature distribution with a small temperature gradient caused by the heat dissipated by the surgical focus on the surgical table. But, that did not disturb the airflow resulting from the natural convection in a significant way.

On the other hand, the airflow on the surgical field presents stagnation and recirculation areas. These phenomena can difficult the removal of particles generated during the surgery and generate discomfort of the surgical team due to no air movement in this place.

Finally, the experimental and numerical results showed that the ventilation system with air supply by one single turbulent diffuser did not present good results in the airflow conditions and, consequently, in the process of removal of pollutants and airborne particles.

7. ACKNOWLEDGEMENTS

Danilo de Moura wish to acknowledge FAPESP and Victor Barbosa Felix, Marcelo Luiz Pereira and Arlindo Tribess wish to acknowledge CNPq for the financial support received.

8. REFERENCES

- Chen, Q., Jiang, Z. and Moser, A., 1992, Control of airborne particle concentration and draught risk in an operating room. "Indoor Air", V.2, pp. 154–167.
- Chow T., T.; Yang, X., Y.; 2003. "Ventilation performance in operating theatres against airborne infection: review of research activities and practical guidance". Division of Buildin Science and Technology, City University, China.
- FLUENT, 2003. "Fluent User's Guide, Version 6.0". Fluent Inc. Lebanon – NH, USA.

- Hartung, C., Kugler, J.; 1998, Perturbations affecting the performance of laminar flow in operating theatres, "15th IFHE Congress", pg. 88-92.
- Kameel, R., Khalil, E., 2003, Predictions of turbulence behavior using k- ϵ model in operating theatres. Mechanical Power Engineering Dpt, Cairo University, Egypt.
- Kao P. H., Yang R. J., 2005. "Virus diffusion in isolation rooms". Department of Engineering Science, National Cheng Kung University, Tainan, Taiwan
- Liu, Y, Moser, A., 2002, Airborne particle concentration control for an operating room, "Proceedings of Roomvent 2002", 8th International Conference, Copenhagen, Denmark, September.
- Liu, Y. ; Moser, A.; Harimoto, K. 2002. "Numerical Study of Airborne Particle Transport in an Operating Room". National Air & Climate Group, Swiss Federal Institute Technology, Switzerland.
- Memarzadeh, F. and Jiang, J., 2001, Methodology for minimizing risk from airborne organisms in hospital isolation rooms. "ASHRAE Trans" 107, pp. 731-747.
- Memarzadeh, F., Manning, A., 2002, Comparison of operating room ventilation systems in the protection of the surgical site. "ASHRAE Trans", 108(2).
- Memarzadeh, F. ; Jiang, Z., 2004. "Effect of Operation Room Geometry and Ventilation System Parameter Variations on the Protection of the Surgical Site". National Institutes of Health, Bethesda, Md.
- Tung, Y., C.; Hu, S., C., 2004. "Flow Fields and Particle Trajectories in Turbulent Type Clean Rooms with Different Supply/Exhaust air Arrangements". Dept of Air Conditioning and Refrigeration Engineering, National Taipei University of Technology, Taiwan.
- Wloszyn M.; Virgone, J.; Mélen S.; 2003. "Diagonal air-distribution system for operating rooms: experiment and modeling". Centre de Thermique de Lyon, France.

9. RESPONSIBILITY NOTICE

The authors are the only responsible for the printed material included in this paper.